INTERNATIONAL JOURNAL ON SMART SENSING AND INTELLIGENT SYSTEMS

Research Article | DOI: 10.2478/ijssis-2026-0025 Issue 1 | Vol. 19 (2026)

Performance Analysis of DWT Based OFDM-IM System in $\alpha-\kappa-\mu$ Fading Environment

Alok Joshi[1], Rachna Singh[1] and Gunjan Gupta[2,*]

[1]Jaypee Institute of Information Technology, Noida, India

[2]Cape Peninsula University of Technology, Cape Town, South Africa

*E-mail: gunjan.gupta12@yahoo.com

Received for publication May 19, 2025.

Abstract

Orthogonal frequency division multiplexing (OFDM) is the most sought choice when it comes to high speed applications owing to its superlative performance in fading environment. However spectral efficiency of OFDM can be further enhanced by using OFDM with index modulation (OFDM-IM) where index of the active subcarrier is also used to carry the payload along with constellation vector. Similar to its predecessor, the OFDM-IM system also suffers from high peak-to-average power ratio. This paper uses discrete wavelet transform (DWT) based OFDM-IM system where the inverse fast Fourier transform (IFFT) block is replaced with DWT block and results show better performance of DWT based systems over IFFT based systems in terms of Peak-to-Average Power Ratio (PAPR) reduction. Besides this we also evaluate the performance of system over $\alpha-\kappa-\mu$ fading channel. $\alpha-\kappa-\mu$ is one of the most sophisticated fading channels which fits very closely to practical data statistics.

Keywords

OFDM, DWT, OFDM-IM, PAPR, $\alpha-\kappa-\mu$

Abbreviations

DFT: Discrete Fourier transform; FBMC: Filter Bank Multi-Carrier; FFT: Fast Fourier Transform; FPGA: Field Programmable Gate Array; IDWT: Inverse Discrete Wavelet Transform; LDPC: Low-Density Parity-Check; MQAM: M-ary Quadrature Amplitude Modulation; NOMA: Non-Orthogonal Multiple Access; QAM: Quadrature Amplitude Modulation; SNR: Signal to Noise Ratio.

I. Introduction

Orthogonal frequency division multiplexing (OFDM) [1, 2] is one of the breakthroughs in implementing high speed data networks & applications. Multiple input Multiple Output (MIMO)-OFDM [1–3] and its variants are still the best candidates in 4G and 5G communications. OFDM supremacy is due to its immunity towards frequency selective fading and inter-symbol interference apart from this cyclic prefix ensures there are no adverse effects of inter-carrier interference (ICI) [4–5].

However, OFDM spectral efficiency can be further enhanced by integrating it with subcarrier index modulation resulting into OFDM with index modulation (OFDM-IM) system. OFDM-IM [6–8] systems are primarily derived from spatial modulation used in MIMO channels. OFDM-IM system not only uses *M-ary* constellation symbols but subcarrier indices too for information transmission. In OFDM-IM system subcarrier indices are activated based on input data stream. Using subcarrier indices for data transmission saves on bandwidth and improves spectral efficiency.

Although OFDM-IM system provides numerous benefits, it is adversely affected due to high peak to average power ratio (PAPR) [9–10]. In time domain high peaks and variation in time domain envelopes

Open Access. Professor Subhas Chandra Mukhopadhyay. CC BY-NC-ND
© 2026 Joshi and Singh, This work is licensed under the Creative Commons Attribution-NonCommercial-NoDerivs 4.0 License https://creativecommons.org/licenses/by-nc-nd/4.0/

are caused due to IFFT taking place at the transmitter. In time domain IFFT sums up the modulated sub-carriers which are aligned in phase generate high peaks leading to large power variations. When such high-power signals pass through high power amplifiers (HPA) used in the downlink, which have non-linearity in its input-output characteristics causes harmonic distortion. High PAPR also causes out of band radiation when it encounters the non-linearity of HPA.

For PAPR reduction, a number of schemes have been suggested in the literature such as *clipping* [11] where envelopes peak beyond a threshold value get clipped off, however non-linearity involved in the operation causes distortion taken care of by *clipping–filtering* [12–13]. *Peak windowing method* [14] works in line with clipping where windowing function is applied to the envelope to hard limit the peaks. *Companding* [15–16] transforms can also be applied on signal envelopes to reduce PAPR, in *peak cancellation and orthogonal peak cancellation* [16–17] method a PAPR reduction waveform is subtracted from OFDM signal for reduction of high peaks. But all the above listed methods improve PAPR performance at the cost of distortion & poor bit error rate (BER) performance.

However, some of the methods are distortion-less such as the scrambling method where multiple representations of the same signal is generated and the one with minimum PAPR is chosen for final transmission. Such methods are *Selective mapping* [18–19] and *Partial transmit sequence* [20–21]. *Tone injection* [22], *Tone reservation* [23], *Active constellation extension* [24] are methods where existing constellation is modified for PAPR reduction. However, additional constellation points result in larger transmission power requirement.

Error control coding methods can also be used for PAPR reduction purpose; however, constructing such codes for a larger set of constellations is complex & tedious. Some of the codes used for PAP reduction purpose are *Reed–Solomon, Golay codes* [25], *Reed-Muller codes* [25], *LDPC codes* [26] and *Turbo codes* [27].

In this paper we have considered OFDM-IM system as it has been proven a better option when it comes to spectral efficiency as compared to conventional OFDM systems. But the IFFT block in the system is replaced by discrete wavelet transform (DWT) block. DWT based OFDM [28] system doesn't require cyclic prefix as DWT has inherent frequency

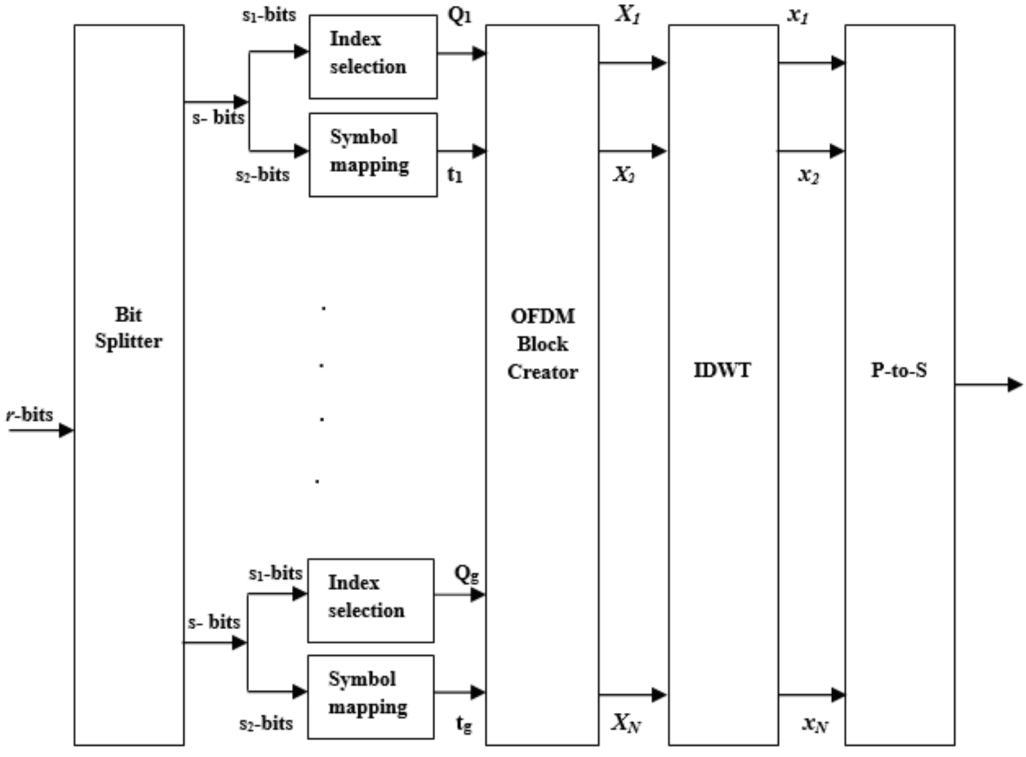


Figure 1: Building blocks of IFFT based OFDM-IM system. IFFT, inverse fast Fourier transform; OFDM, orthogonal frequency division multiplexing; OFDM-IM, OFDM with index modulation.

time synchronization. So in terms of complexity & spectral efficiency DWT based systems are better since cyclic prefix reduces spectral efficiency too. Low side lobe levels in DFT are also one of the reasons why they have better PAPR performance than IFFT based systems. For performance analysis we have simulated the system considering $\alpha-\kappa-\mu$ fading environment [29]. Since multipath phenomenon leads to fading and among all the available mathematical distributions $\alpha-\kappa-\mu$ is universally accepted as the most flexible distribution which optimally fits into the practical statistical data set.

II. OFDM-IM System Model

System block diagram of IFFT based OFDM-IM system is given in Figure 1. The input bit stream of *r* bits is divided in *g* groups, with each group carrying *s* bits such that $g=\frac{m}{s}$. Let *N* be the number of subcarriers in each OFDM symbol, these subcarriers are also divided in *g* subgroups with each having $p=\frac{N}{g}$ subcarriers. In each of these subgroups only a fraction of *k* subcarriers are active and rest of the *p-k* are inactive.

Only the active subcarriers carry the constellation mapped symbols while inactive ones do not carry any data with them.

In each subgroup s_1 bits are used for selection of *k* active subcarriers from a pool of *p* and s_2 bits which are used for constellation mapping of *M-ary* modulated signal. Where:

$$s=s_1+s_2$$

$$s_1=\lfloor \log_2 C(p,k) \rfloor$$

$$s_2=k\ \log_2 M$$

So information is transmitted by active subcarrier indices and the symbol mapped of *M-ary* modulated signal carried by these active subcarriers, thus achieving data rate of $k\log_2 M+\lfloor \log_2 C(p,k) \rfloor$ bits per subgroup or OFDM subblock. The overall data rate would be -

$$s_1 g+s_2 g=g\left[k\log_2 M+\lfloor \log_2 C(p,k) \rfloor\right]$$

Unused subcarriers can be used for transmitting additional information in spatial domain. For each subgroup *j = 1,2….g* the active subcarrier indices are represented as $Q_j=\{Q_j^1,Q_j^2.....Q_j^k\}$. Whereas in Q^a, *a* represents the active subcarrier.

The output of the symbol mapper is represented as:

$$t_j^{\alpha}=\{t_j^1,t_j^2....,t_j^k\}$$

Where $t_j^{\alpha}\in T$, for *j = 1, 2….g* and *a = 1, 2...,k*. *T* represents the symbol set which are transmitted using *k* active subcarriers, considering each of the OFDM subblock is normalized to unity power i.e. $E\{t_j t_j^H\}=k$. (.) & $(.)^H$ represents *Hermitian transpose*. For *p = 4 & k = 2 the subblocks* can be created as follows:

Bits {0,0} ***Active subcarrier indices*** {1, 2} ***subblocks*** $\{t^1,t^2,0,0\}$
Bits {0,1} ***Active subcarrier indices*** {2, 3} ***subblocks*** $\{0,t^2,t^3,0\}$
Bits {1,0} ***Active subcarrier indices*** {3, 4} ***subblocks*** $\{0,0,t,^3,t^4\}$
Bits {1,1} ***Active subcarrier indices*** {1, 4} ***subblocks*** $\{t^1,0,0,t^4\}$

With the help *Qj* & t_j the OFDM block creator generates the output given by

$$X_F=[X_1,X_2.....X_N]^T$$

Since carrier wither carries a *0* or symbol thus $X_i\in\{T,0\}$ for *i = 1, 2…N*. After performing *IFFT* operation we get:

$$x_\gamma=\frac{N}{\sqrt{M}}IFFT\{X_F\}=\frac{1}{\sqrt{M}}W_N^H X_F$$

Where *M* is the number of OFDM symbols, x_γ is time domain OFDM block, *W* represents *DFT* matrix & $W_N^H W_N=N$ and $\frac{N}{\sqrt{M}}$ is scaling factor for normalization $E\{x_\gamma^H x_\gamma\}=N$. After IFFT cyclic prefix is placed at the beginning of OFDM block. Finally parallel to serial convertor & D/A conversion takes place.

III. DWT Based OFDM-IM System Model

DWT based OFDM-IM system given in Figure 2 where IFFT block is replaced by DWT. In DWT signal is decomposed into basic functions which are called wavelets, they can be assumed as oscillatory shapes. Wavelet allows easier representation

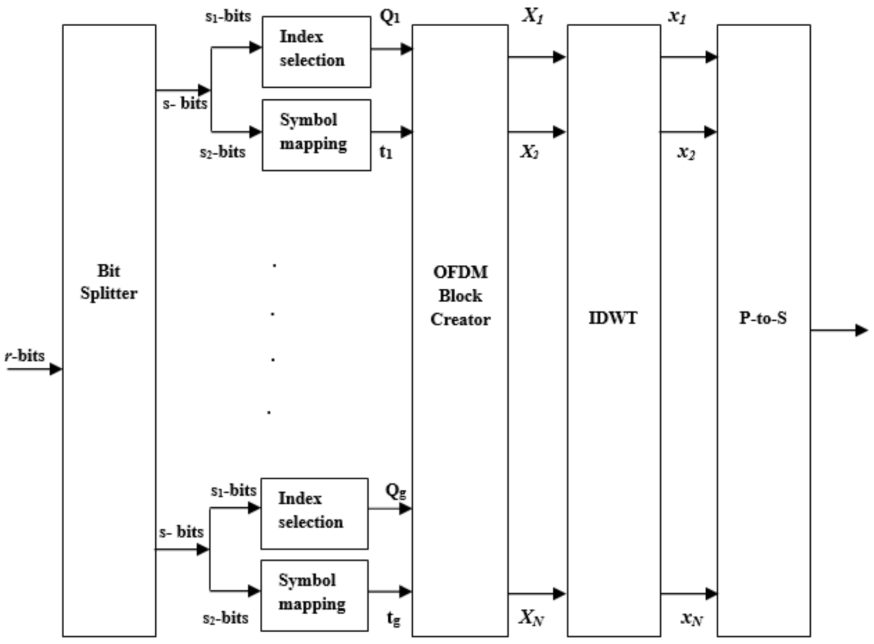


Figure 2: Building blocks of DWT based OFDM-IM system. DWT, discrete wavelet transform; OFDM, orthogonal frequency division multiplexing; OFDM-IM, OFDM with index modulation.

of unpredictable signals than Fourier analysis. In contrast to Fourier, here signal generated using fixed wavelet function rather than trigonometric functions.

Replacing IFFT/FFT Blocks with IDWT/DWT blocks leads to better spectral efficiency of DWT based OFDM-IM system as there is no need of cyclic prefix insertion. This advantage in spectral efficiency does not hamper BER performance of the system. In the presence of noise effecting phase of signal DWT based OFDM system performs better than conventional IFFT based OFM system [30]. As far as PAPR performance is concerned, DWT based OFDM system outperforms IFFT based OFDM system.

DWT generates wavelet carriers which are orthogonal and completely replaces time domain windowed complex terms generated from IFFT operation. If A & B are time location and scale index respectively, to ensure orthogonality between A & B using time frequency localization, the mother wavelet χ is defined as:

$$\chi_{A,B}(t) = 2^{-A/2}\,\chi(2^{-A}t - B) \quad \text{\& to ensure orthogonality}$$

$$\chi_{A,B}(t), \chi_{m,n}(t) = 1 \;\; if \;\; A = m \;\; and \;\; B = n = 0 \qquad otherwise$$

The DWT OFDM symbol $a(t)$ represented as:

$$a(t) = \sum_{A \le \Re} \sum_{B} U_{A,B}(t)\,\chi_{A,B}(t) + \sum O_{A,B}\,\rho_{\Re,A}(t)$$

Where $\rho_{\Re,A}(t)$ is scaling function, $O_{A,B}$ are approximation coefficients, $U_{A,B}$ Wavelet coefficients, $\Re$ scale with best frequency localization of carriers.

IV. Computational Complexity

Let DWT is using up-sampling factor of 2 with wavelet coefficients $U_{A,B}$ and approximation coefficients $O_{A,B}$. Then the number of complex multiplications and additions will be $2\frac{N}{2}\log_2 N$ and $N\log_2 N$ respectively, thus the order of complexity will be $O(N\log_2 N)$

FFT based OFDM systems have similar order of complexity but in DWT based overall system complexity decreases with removal of cyclic prefix.

V. Peak to Average Power Ratio

IFFT sum used at the transmitter may result into high peaks in the OFDM signal envelope. For an OFDM signal with N subcarrier the PAPR is given as:

$$PAPR(x) = \frac{\max_{0<n<N-1} |x_n|^2}{E\left[|x_n|^2\right]}$$

Table 1: Values of α, κ and μ for various fading distribution

Sl. No.	Distribution	α	κ	μ
1	Rayleigh	2	0	1
2	Rician	2	1	1
3	Nakagami-m	2	0	<1
4	Gaussain	2	0	0.5
5	Weibull	3.5	0	1

VI. $\alpha-\kappa-\mu$ Fading Environment

A variety of channel distribution functions are available to characterize the wireless channel. One of the best suited fading models for practical statistical data is $\alpha-\kappa-\mu$. The values of α, κ and μ for various fading distribution is shown in

$$PAPR(x)=\frac{\max_{0<n<N-1}|x_n|^2}{E[|x_n|^2]}$$

In non-homogenous scattering conditions the $\alpha-\kappa-\mu$ fading model is used for representing signal variations. As per Table 1, this model includes all the possible small-scale signal fading models. The p.d.f for the model is given as:

$$f_R(r)=\left[\frac{\alpha\,\mu(1+\kappa)^{\frac{1+\mu}{2}}\,\kappa^{\frac{1-\mu}{2}}}{e^{\mu\kappa}}\right]\left[\frac{r}{\tilde{r}}\right]^{\frac{\alpha(\mu+1)}{2}-1}\times e^{-\left[\mu(1+\kappa)\left(\frac{r}{\tilde{r}}\right)^{\alpha}\right]}I_{\mu-1}(2\mu\sqrt{\kappa(1+\kappa)})\left(\frac{r}{\tilde{r}}\right)^{\alpha/2}$$

Where: α = non-linearity of multipath

κ = ratio of dominant power component to total power of scattered components

μ = Number of multipath channels

$\tilde{r}=\sqrt{E(Y^2)}$ is the rms value of *signal envelope Y*

$I_e(.)$ = Modified Bessel's function of the first kind and order *e*.

VII. Performance Analysis in $\alpha-\kappa-\mu$ Fading Environment

Average value of received signal to noise ratio for $\alpha-\kappa-\mu$ channel $\tilde{\xi}=E[H^2]\frac{E_s}{N_0}$ (Average SNR) for bit energy E_b it can be written as $\tilde{\xi}=E[H^2]\frac{\kappa E_b}{N_0}$ Where E_s is symbol energy, H channel coefficients. The distribution of received signal will be:

$$f(\xi)=\left[\frac{\alpha\,\mu(1+\kappa)^{\frac{1+\mu}{2}}}{2\kappa^{\frac{\mu-1}{2}}e^{\mu\kappa}\tilde{\xi}^{\frac{\alpha(\mu+1)}{4}}}\right]\left(\xi^{\frac{\alpha(\mu+1)}{4}-1}\right)\times e^{-\left[\mu(1+\kappa)\left(\frac{\xi}{\tilde{\xi}}\right)^{\frac{\varepsilon}{2}}\right]}I\left[2\mu\sqrt{\kappa(1+\kappa)}\left(\frac{\xi}{\tilde{\xi}}\right)^{\frac{\alpha}{4}}\right]$$

The BER equation for the M-QAM signaling is given by [25]

$$P_e=\frac{3}{n}\left(1-\frac{1}{\sqrt{M}}\right)Q\left(\sqrt{\frac{3}{M-1}\tilde{\xi}}\right)\text{ where }n=\log_2 M$$

For a system with a number of signal constellation points $Z_1=(M)^{Z_2}$ it can be given as $\alpha-\kappa-\mu$ for fading environment as

$$P_e=\frac{3}{n}\left(1-\frac{1}{\sqrt{M}}\right)\sum_{j_1}^{Z_1}\sum_{j_2}^{Z_1}\frac{Z(j_1,j_2)}{Z_1\log Z_1}\times\int_0^{\infty}Q\left(\sqrt{\frac{3.\kappa.\frac{E_b}{N_0}\xi}{M-1}}\right)f(\xi).d\xi$$

Where $Z(j_1, j_2)=1,\quad if\quad j_1=j_2$

VIII. Results

The parameters used for PAPR calculations are given in Table 2.

The PAPR comparison of both the systems is done by simulating complementary cumulative distribution function (CCDF). CCDF curve suggests that

Table 2: Simulation parameters for OFDM-IM system

Sl. No.	Distribution	FFT based system	DWT based system
1	Number of symbols	10,000	10,000
2	FFT/DWT size	64	-
3	Modulation	M-QAM	M-QAM
4	Subcarriers	512	512
5	Cyclic prefix duration	0.8 μs	-
6	Sampling frequency	20 MHz	
7	Total symbol duration	4 μs	
8	Subcarrier index	–26 to –1; +1 to +26	
9	Subcarrier spacing	312.5 KHz	
10	Mapping scheme	8-QAM	

DWT, discrete wavelet transform; OFDM, orthogonal frequency division multiplexing; OFDM-IM, OFDM with index modulation.

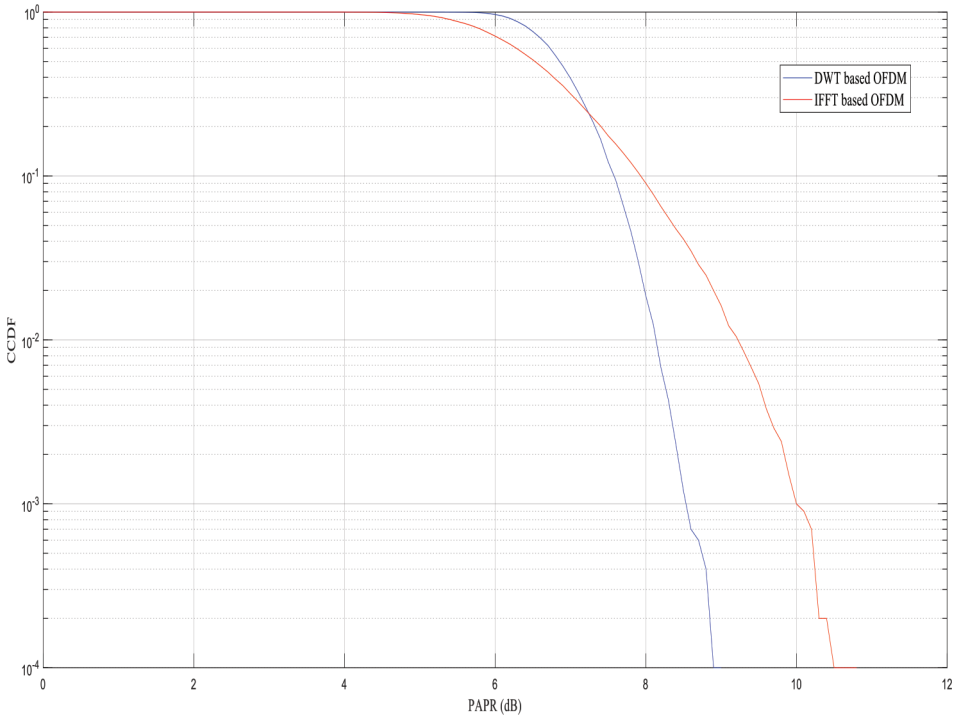


Figure 3: CCDF curves for FFT & DWT based OFDM-IM system. CCDF, complementary cumulative distribution function; DWT, discrete wavelet transform; IFFT, inverse fast Fourier transform; OFDM, orthogonal frequency division multiplexing; OFDM-IM, OFDM with index modulation.

DFT based systems gives better performance than FFT based systems. Simulation curves for the CCDF are given n Figure 3. This clearly indicates that PAPR value of DWT based system is around 8.5 dB whereas for FFT based OFDM system it is around 11 dB.

BER for 8-QAM system is simulated for $\alpha = 2, \kappa = 0, \mu = 1$ and $\alpha = 2, \kappa = 0, \mu = 0.5$, the BER curves are shown in Figure 4.

Figure 4 suggests BER performance for $\alpha = 2, \kappa = 0, \mu = 1$ (Rayleigh) is inferior to

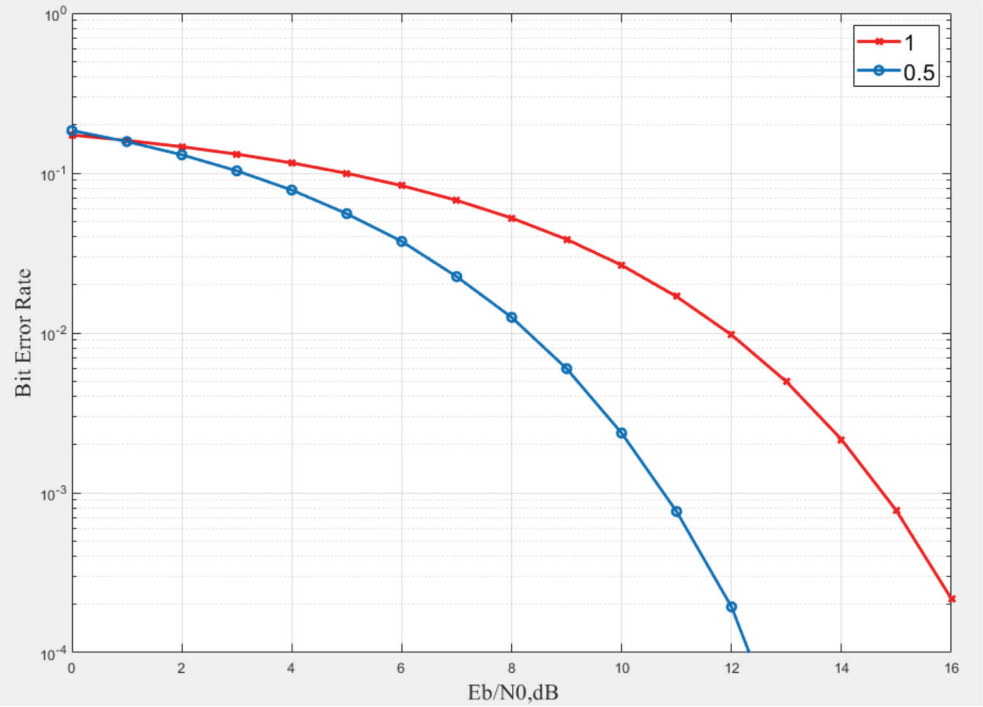


Figure 4: BER curves for $\alpha = 2, \kappa = 0, \mu = 1$ and $\alpha = 2, \kappa = 0, \mu = 0.5$. BER, bit error rate.

$\alpha = 2, \kappa = 0, \mu = 0.5$ (Nakagami) which satisfy the general convention.

DWT-based OFDM-IM systems show better spectral efficiency and PAPR performance compared to FFT-based OFDM setups. You know how narrowband interference works. DWT handles it better than traditional methods, along with reducing ICI issues.

Looking at computational complexity, FFT-based systems for N-subcarrier OFDM require operations on the order of $N.\log_2 N$. Meanwhile DFT-based approaches only need order N operations. That's a clear advantage for resource usage. DWT itself is already widely used in signal processing circles, so scaling up deployments shouldn't pose major hurdles.

Power consumption differences matter here. FFT implementations typically demand high-power DSP or FPGA processors. DFT alternatives can run on lower-power chipsets instead. Though wavelet selection sometimes complicates DFT implementations more than expected. There's always a trade-off between spectral efficiency gains and practical implementation challenges.

Comparing DWT-OFDM IM against NOMA and FBMC approaches brings more insights. Both FBMC and DWT-OFDM skip cyclic prefixes entirely, freeing up bandwidth for actual data transmission. They're also more resilient against narrowband interference situations people often see in crowded spectrum areas. But FBMC runs into headaches with MIMO configurations due to requiring multiple filter banks in hardware setups.

NOMA's non-orthogonal nature does boost system capacity and latency metrics significantly on paper. Spectral efficiency looks great in simulations too. The catch comes during real-world deployment though—receiver designs get super complex fast when channel conditions aren't perfect. Even minor distortions can throw off the whole decoding process pretty hard you know.

IX. Conclusion

The paper evaluates the PAPR performance of the DWT based OFDM-IM systems and suggests performance improvement over existing FFT based systems. Using the DWT based system decreases the system complexity. OFDM-IM systems are themselves more spectrum efficient than conventional OFDM systems. Paper also evaluated system performance in $\alpha - \kappa - \mu$ fading environment, which is one of the most sought-after choices for real world data in wireless communication. BER performance curves comply with the literature too. DWT based

OFDM-IM systems are one of the strong candidates for next generation wireless communication owing to its enhanced spectral efficiency and lower complexity. OFDM acts as a strong pillar to support 4G and 5G technologies and $\alpha - \kappa - \mu$ fading environment is the most sophisticated model for real time scenario. DWT based IM-OFDM enhances conventional OFDM capabilities in terms of improved spectral efficiency and PAPR performance.

References

[1] W. Gao and X. Kuai, "Joint Impulsive Noise and Narrowband Interference Mitigation in Time-Varying OFDM Communications," in *IEEE Communications Letters*, Jan 2025 [Early access]

[2] B. Ren, K. C. Teh, H. An and E. Gunawan, "MIMO-OFDM Modulation Classification Using 4D2DConvNet for 5G Communications," in *IEEE Wireless Communications Letters*, vol. 13, no. 7, pp. 1883-1887, July 2024

[3] J. Wang and M. Kaneko, "Exploiting Beam Split-Based Multi-User Diversity in Terahertz MIMO-OFDM Systems," in *IEEE Wireless Communications Letters*, vol. 14, no. 1, pp. 28-32, Jan. 2025.

[4] J. -H. Park, Y. -J. Yoon, W. Cho, D. Ham and S. -C. Kim, "Intercarrier Interference Mitigation for Communication Compatible OFDM Radar," in IEEE Transactions on Vehicular Technology, vol. 73, no. 4, pp. 5930-5934, April 2024

[5] Z. Xiao, S. Fu, S. Yao, M. Tang, P. Shum and D. Liu, "ICI Mitigation for Dual-Carrier Superchannel Transmission Based on m-PSK and m-QAM Formats," in Journal of Lightwave Technology, vol. 34, no. 23, pp. 5526-5533, 1 Dec.1, 2016.

[6] S. Choi and H. Park, "Reed-Muller Code-Based Index Codebook Design for Dual-Mode OFDM-IM," in IEEE Access, vol. 13, pp. 37924-37930, 2025.[early access]

[7] J. Hu, Y. Wang, Z. Lian, Y. Su and Z. Xie, "Optimal OFDM-IM Signals With Constant PAPR," in IEEE Transactions on Broadcasting, vol. 70, no. 3, pp. 945-954, Sept. 2024

[8] A. Tusha, S. Doğan and H. Arslan, "A Hybrid Downlink NOMA With OFDM and OFDM-IM for Beyond 5G Wireless Networks," in IEEE Signal Processing Letters, vol. 27, pp. 491-495, 2020

[9] Y. Chang and K. Fukawa, "PAPR Reduction for OFDM Mobile Wireless Communications by Constant-Amplitude Signal Decomposition," in IEEE Access, vol. 13, pp. 54672-54685, 2025.

[10] J. Hu, Y. Wang, Z. Lian, Y. Su and Z. Xie, "Low-Complexity PAPR Reduction of OFDM-IM Signals via ADMM Approaches," in IEEE Communications Letters, vol. 28, no. 5, pp. 1161-1165, May 2024.

[11] Z. Xing, K. Liu, A. S. Rajasekaran, H. Yanikomeroglu and Y. Liu, "A Hybrid Companding and Clipping Scheme for PAPR Reduction in OFDM Systems," in IEEE Access, vol. 9, pp. 61565-61576, 2021

[12] Y. Sun and H. Ochiai, "Maximum-Likelihood-Based Performance Enhancement of Clipped and Filtered OFDM Systems With Clipping Noise Cancellation," in IEEE Wireless Communications Letters, vol. 11, no. 3, pp. 448-452, March 2022.

[13] S. Gökceli et al., "Novel Iterative Clipping and Error Filtering Methods for Efficient PAPR Reduction in 5G and Beyond," in IEEE Open Journal of the Communications Society, vol. 2, pp. 48-66, 2021

[14] K. Humse and C. Anjanappa, "Comparative Analysis of PAPR Reduction Method using Windowing Technique and Digital Predistortion Technique for OFDM Systems," in proceedings of IEEE International Conference on Recent Advances in Science and Engineering Technology (ICRASET), India, 2024, pp. 1-5

[15] K. Liu, X. Cui, Z. Xing and Y. Liu, "Generalized Continuous Piecewise Linear Companding Transform Design for PAPR Reduction in OFDM Systems," in IEEE Transactions on Broadcasting, vol. 68, no. 3, pp. 780-796, Sept. 2022.

[16] M. Davoodabadi, M. Shamsi and F. Marvasti, "Orthogonal Peak Cancellation: A Bandwidth-Efficient Companding Method for PAPR Reduction in OFDM," in IEEE Communications Letters, vol. 29, no. 6, pp. 1491-1494, June 2025

[17] Z. Li, R. Nojima, O. Muta, M. Omoto, T. Makita and K. Maruta, "In-Band Distortion Compensation for Peak Cancellation-Based PAPR Reduction in Massive MIMO-OFDM With Uniform Planar Array," in IEEE Access, vol. 12, pp. 156118-156130, 2024.

[18] A. Kumar, N. Gaur and A. Nanthaamornphong, "Optimizing PAPR, BER, and PSD Efficiency: Using Phase Factors Generated by Bacteria Foraging Algorithm for PTS and SLM Methods," in IEEE Access, vol. 12, pp. 54964-54977, 2024.

[19] S. -Y. Zhang and B. Shahrrava, "A SLM Scheme for PAPR Reduction in Polar Coded OFDM-IM Systems Without Using Side Information," in IEEE Transactions on Broadcasting, vol. 67, no. 2, pp. 463-472, June 2021.

[20] T. Khai Nguyen, E. Bedeer, H. H. Nguyen, J. Eric Salt and C. Howlett, "Optimized Canceling

Signals for PTS Schemes to Improve the PAPR of OFDM Systems Without Side Information," in IEEE Transactions on Broadcasting, vol. 71, no. 1, pp. 360-370, March 2025

[21] S. -Y. Zhang, B. Shahrrava, Y. -X. Zhang and Z. -H. Zhuo, "A Permutated Partial Transmit Sequence Scheme for PAPR Reduction in Polar-Coded OFDM-IM Systems," in IEEE Transactions on Vehicular Technology, vol. 72, no. 12, pp. 15867-15881, Dec. 2023.

[22] M. Hu, W. Wang, W. Cheng and H. Zhang, "Initial Probability Adaptation Enhanced Cross-Entropy-Based Tone Injection Scheme for PAPR Reduction in OFDM Systems," in IEEE Transactions on Vehicular Technology, vol. 70, no. 7, pp. 6674-6683, July 2021.

[23] Y. Liu, F. Cheng, J. Yi, Y. Rao and X. Wan, "PAPR and Sidelobe Reduction Using Tone Reservation in OFDM RadCom Systems," in IEEE Sensors Journal, vol. 24, no. 16, pp. 26645-26658, 15 Aug.15, 2024.

[24] Y. Liu, Y. Wang and B. Ai, "An Efficient ACE Scheme for PAPR Reduction of OFDM Signals With High-Order Constellation," in IEEE Access, vol. 7, pp. 118322-118332, 2019.

[25] J. A. Davis and J. Jedwab, "Peak-to-mean power control in OFDM, Golay complementary sequences, and Reed-Muller codes," in IEEE Transactions on Information Theory, vol. 45, no. 7, pp. 2397-2417, Nov. 1999.

[26] O. Daoud and O. Alani, "Reducing the PAPR by utilisation of the LDPC code," in IET Communications, vol. 3, no. 4, pp. 520-529, April 2009.

[27] M. Sabbaghian, Y. Kwak, B. Smida and V. Tarokh, "Near Shannon Limit and Low Peak to Average Power Ratio Turbo Block Coded OFDM," in IEEE Transactions on Communications, vol. 59, no. 8, pp. 2042-2045, August 2011.

[28] M. Wils, M. Sharma and M. Moonen, "Per-Wavelet Equalization for Discrete Wavelet Transform Based Multi-Carrier Modulation Systems," in IEEE Open Journal of Signal Processing, vol. 4, pp. 52-60, 2023

[29] S. Tated, G. Anand and D. Sadhwani, "Simplified SEP Approximations of Coherent Digital Modulation Schemes over alpha-kappa-mu Fading Channel," in IEEE Latin America Transactions, vol. 22, no. 7, pp. 566-573, July 2024.

[30] A. Joshi, A. Manas, S. Garg, R. Wason, R., "PAPR Reduction Comparison in FFT-Based OFDM versus DWT-Based OFDM", In: Rawat, B., Trivedi, A., Manhas, S., Karwal, V. (eds) Advances in Signal Processing and Communication. Lecture Notes in Electrical Engineering, vol 526, 2019, Springer, Singapore. https://doi.org/10.1007/978-981-13-2553-3_11